

## Surface morphology and growth of AgBr on Ag(111)

M. K. Wagner, J. C. Hansen,\* R. deSouza-Machado, S. Liang, and J. G. Tobin<sup>†</sup>  
*Department of Chemistry, University of Wisconsin-Madison, Madison, Wisconsin 53706*

M. G. Mason, S. Brandt, and Y. T. Tan  
*Research Laboratories, Eastman Kodak Company, Rochester, New York 14650*

A.-B. Yang and F. C. Brown  
*Department of Physics, University of Washington, Seattle, Washington 98195*  
(Received 8 October 1990)

Angle-resolved photoemission with synchrotron radiation has been used to probe the surface morphologies of AgBr deposited by molecular-beam epitaxy onto Ag(111), as a function of coverage and substrate temperature. Depositions performed at 130°C yield results consistent with a Stranski-Krastanov (SK) growth, whereas surfaces prepared at liquid-nitrogen temperatures exhibit a more nearly layer-by-layer growth. These interpretations are supported by core-level and valence-band studies, which probed the binding energies and intensities of the Br 3*d* core level and the Ag(111) surface state. Low-energy electron diffraction observations show the initial SK layer to have a  $(\sqrt{3} \times \sqrt{3})R30^\circ$  structure, while heavier depositions exhibit indications of AgBr(111) islands. Cold depositions show no long-range order. Surface morphology changes induced by warming a cold deposition were also studied.

### I. INTRODUCTION

Silver halides, central to the photographic industry because of their photosensing capabilities, have been the subject of many investigations. However, understanding the relationship between both electronic and geometrical structure and the interaction of these materials with light remains a topic of current research and ongoing debate.<sup>1,2</sup> For example, typical fast photographic negative emulsions contain tabular grains of AgBr(111), and it is believed that latent image formation occurs at the surfaces of these structures.<sup>3</sup> Consequently, it is important not only to study bulk properties of AgBr(111), but also to investigate its surface, including both changes in electronic structure and possible surface reconstructions. Surface reconstruction seems likely because a simple truncation of the AgBr lattice along the (111) direction results in a surface plane of either all Ag or all Br atoms. Since these atoms carry a net positive or negative charge, respectively, reconstruction is expected in order to reduce this large surface free energy. To effectively study these surface phenomena, it is necessary to prepare a AgBr(111) surface whose ordering and surface morphology are well known.

To this end, we have performed an extensive study of AgBr deposited on Ag(111) using angle-resolved photoemission spectroscopy (ARPES) and low-energy electron diffraction (LEED). AgBr was previously shown to grow in a (111) orientation when heavily deposited onto Ag(111) at 130°C, although the actual structure and intermediate growth of the surfaces prepared were not studied.<sup>4</sup> By incrementally increasing the AgBr coverage from the monolayer regime until bulklike samples were obtained, we were able to separate contributions, deter-

mine growth modes, and gain insight into the surface structure. Moreover, this growth and morphology information is important not only for the understanding of the AgBr/Ag(111) surface, but also as a general example of the growth of an ionic material on a metal substrate.

We have studied AgBr deposited on Ag(111) as a function of coverage and temperature, and our conclusions about its surface morphologies and growth are the following. (i) At substrate temperatures of 130°C, AgBr growth occurs in a Stranski-Krastanov (SK) manner, i.e., a well-ordered  $(\sqrt{3} \times \sqrt{3})R30^\circ$  layer is formed at a low break-point coverage, followed by the formation of islands consistent with AgBr(111) at higher coverage. (ii) When samples are prepared at liquid-nitrogen temperatures, AgBr growth appears to be more nearly layer-by-layer but shows no evidence of long-range order. (iii) An overlayer prepared cold, when allowed to warm, appears to first form the thin  $(\sqrt{3} \times \sqrt{3})R30^\circ$  layer with weakly ordered islands at room temperature. This is followed by the continued coalescence and ordering of the islands at higher temperatures, until by 130°C, the results are consistent with surfaces prepared directly at that temperature.

### II. EXPERIMENT

These experiments were carried out in a spectrometer<sup>5</sup> equipped to perform ARPES, Auger-electron spectroscopy (AES), LEED, residual gas analysis and vapor depositions, all under ultrahigh vacuum conditions. The photoemission measurements were made at the University of Wisconsin Synchrotron Radiation Center (UWSRC) on the 1-GeV ring, Aladdin, using the University of Illinois Extended Range Grasshopper (ERG) and the UWSRC

6 m Toroidal Grating Monochromator (TGM). The combined resolution of the monochromator and the electron energy analyzer was 0.14 eV at  $h\nu = 55$  eV and 0.24 eV at  $h\nu = 120$  eV for the growth experiments at 130 and  $-190^\circ\text{C}$  performed on the ERG, and was 0.22 eV at  $h\nu = 120$  eV for the annealing experiment performed on the TGM. The Ag(111) substrate was cleaned with successive cycles of Ar ion bombardment and annealing to  $400^\circ\text{C}$ . The cleanliness and ordering of the Ag(111) surfaces prepared were confirmed with AES, LEED, and by observation of the presence of the Ag(111) surface state using ARPES.

Depositions were performed *in situ* by resistively heating AgBr wrapped in Pt wire in a shuttered assembly. These depositions were monitored with a quartz-crystal microbalance and the chamber pressure was  $\leq 9 \times 10^{-10}$  torr during evaporation. All coverages are expressed in terms of the spectroscopically determined SK break-point coverage, to which we have assigned by definition a value of  $\Theta = 1$ . An absolute determination of this break-point coverage was attempted *ex situ*, using *in vacuo* deposition and external neutron activation measurement of the amount of AgBr deposited onto either glass or SiN<sub>2</sub>. However, a precise value was not obtained. The amount of Ag at the SK break point was determined to be equivalent to  $0.41 \pm 0.41$  monolayer (ML) of Ag(111), the most reliable sample giving a result of 0.42 ML of Ag(111). The necessity of performing the neutron activation depositions onto different substrates also introduces questions of relative sticking coefficients and sublimation rates. Although imprecise, it is very useful to have an independent indication that the break point occurs at depositions corresponding to an amount of Ag equivalent to 1 ML or less of Ag(111). Additionally, it is very useful to compare these results with our observations at the break point of a  $(\sqrt{3} \times \sqrt{3})R30^\circ$  LEED pattern which suggests a coverage of  $\frac{1}{3}$  ML. However, we cannot rule out the other possibilities, such as a  $\frac{2}{3}$  ML coverage being associated with the  $(\sqrt{3} \times \sqrt{3})R30^\circ$  LEED pattern.

To minimize probe-induced damage, all AgBr samples were cooled to liquid-nitrogen temperatures during photoemission and LEED measurements. This cooling substantially slows interstitial Ag<sup>+</sup> migration, thus inhibiting latent-image formation associated with Ag atom clustering.<sup>3,6</sup> Although the effectiveness of this procedure had been demonstrated for photoemission,<sup>4</sup> LEED measurements had never been previously attempted, and therefore samples probed by LEED were never subsequently used for photoemission. However, no detrimental effects were observed due to the low-current, low-energy (0.8–2.0  $\mu\text{A}$ , 50–200 eV) electron beam. Attempts to perform AES (30  $\mu\text{A}$ , 2000 eV), on the other hand, produced a significant degradation of LEED patterns.

Degradation of the samples by background gases also was not a problem. During our experiments, the vacuum was typically in the  $10^{-10}$  torr range, although occasionally the pressure rose into the  $10^{-9}$  torr range when samples cooled to  $-190^\circ\text{C}$  were returned to room temperature. It is interesting to note that the AgBr overlayers prepared at  $130^\circ\text{C}$  showed a remarkable resistance to

adsorption-induced change as evidenced by valence-band and core-level photoemission. Even after an exposure to atmospheric pressure, little change could be seen in spectral features. The exposed sample was not used for subsequent experimentation.

The bulk of the remainder of this paper will discuss the growth and surface morphology studies of AgBr depositions (a) prepared at  $130^\circ\text{C}$ , (b) prepared at  $-190^\circ\text{C}$ , and (c) prepared at  $-190^\circ\text{C}$  followed by stepwise annealing to  $130^\circ\text{C}$ . This will be followed by a brief conclusion.

### III. RESULTS AND DISCUSSION

#### A. Deposition at $130^\circ\text{C}$

When AgBr is deposited on Ag(111) at  $130^\circ\text{C}$ , the core-level and valence-band photoemission results are consistent with Stranski-Krastanov growth. In this model, a thin, two-dimensional layer is formed followed by subsequent island growth. Figure 1(a) contains ARPES spectra of the Br  $3d_{5/2,3/2}$  core levels with increasing AgBr coverage, deposited at  $130^\circ\text{C}$ . The spectra were taken at  $h\nu = 120$  eV to maximize surface sensitivity. Initially, only a single pair of spin-orbit-split peaks is observable at  $B^F$  (binding energies with respect to the silver Fermi level) =  $67.97 \pm 0.06$  and  $69.02 \pm 0.06$  eV. At coverages above  $\Theta = 1$ , an additional feature grows in at higher binding energy,  $B^F = 69.85 \pm 0.04$  eV. The "three-line" spectrum observed at these higher coverages is actually an overlapping of two spin-orbit-split doublets differing in binding energy by  $\sim 0.8$  eV. The lower binding energy doublet is associated with the initial SK layer, and the higher binding energy doublet with islands. Based on the literature concerning AgBr growth at this temperature,<sup>7</sup> and on LEED observations (discussed below), these islands appear to be AgBr(111). The binding energies of all three peaks remain nearly constant within 0.1 eV over all coverage ranges. While the width of the SK component remains constant at 0.35 eV, the width of the island component increases slightly to 0.41 eV at higher coverages, possibly indicating the formation of surface and bulk contributions.

An analysis of the normal emission intensities of these core levels, as shown in Fig. 1(b), is strongly supportive of the SK growth model. At low coverages the integrated intensity from the Br  $3d$  levels increases linearly as the initial SK layer is formed. At higher coverages the total intensity remains nearly constant as the additional AgBr goes into island growth, leaving a substantial portion of the initial SK layer uncovered. This behavior of integrated, total intensity is identical to that observed for Auger intensities in systems that exhibit SK growth.<sup>8</sup> A sharp break in slope occurs between these two regions at the point where the SK layer is completed. We have assigned this point the value  $\Theta = 1.0$  and all depositions are expressed relative to it. (As discussed above, it seems highly probable that the  $\Theta = 1.0$  point corresponds to a deposition of less than or equal to a Ag(111) monolayer, and it is likely that the coverage is actually about  $\frac{1}{3}$  ML.) Moreover, further support of the SK growth is seen in an

analysis of the area of the lowest binding energy peak ( $B^F \approx 68$ ), which is associated with the SK layer only and has no overlap with the island components. It shows a similar linear growth to  $\Theta=1$ , and then a very slow attenuation as the layer is covered by islands. Off-normal emission results are also consistent with the hypothesis of a SK growth mode.<sup>9</sup>

The existence of island structures is seen with scanning

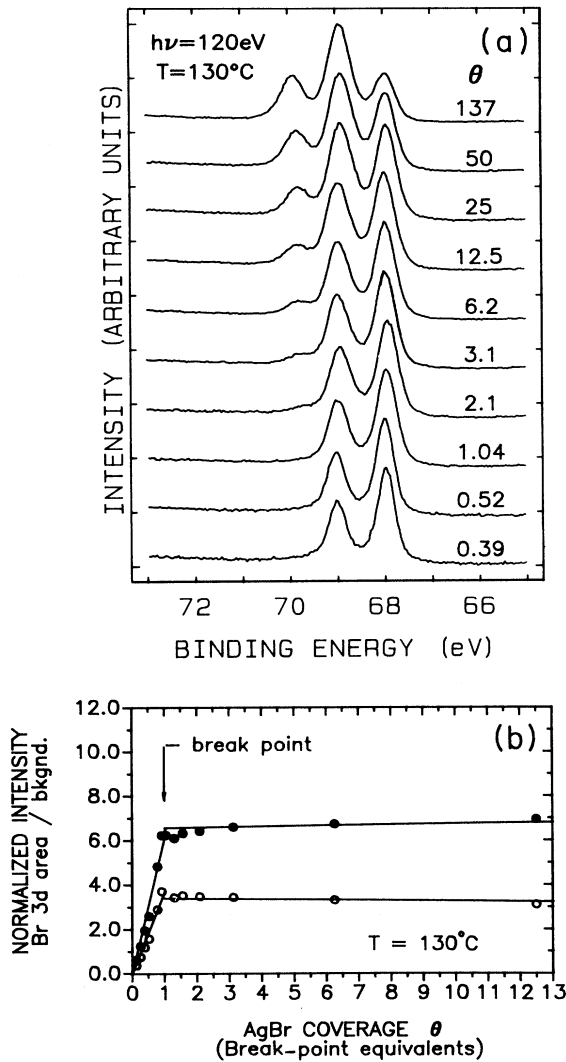


FIG. 1. Br 3d core-level results for AgBr/Ag(111) samples prepared at 130°C. (a) Normal emission ARPES spectra of the Br  $3d_{5/2,3/2}$  core levels taken at  $h\nu=120$  eV.  $\Theta$  indicates coverage relative to the SK break-point value. The polarization of the light lay in the plane containing the surface normal and  $[1\bar{1}0]$ , with an angle of incidence of  $60^\circ$  relative to the surface normal. (b) A plot of total Br 3d ( $\bullet$ ) and SK component  $3d_{5/2}$  ( $\circ$ ) integrated intensity as a function of coverage at 130°C. The SK break point is indicated. Although data for coverages up to  $\Theta=137$  were used to determine the post-break-point line, points beyond  $\Theta=13$  are not shown to allow the break-point region to be clearly presented.

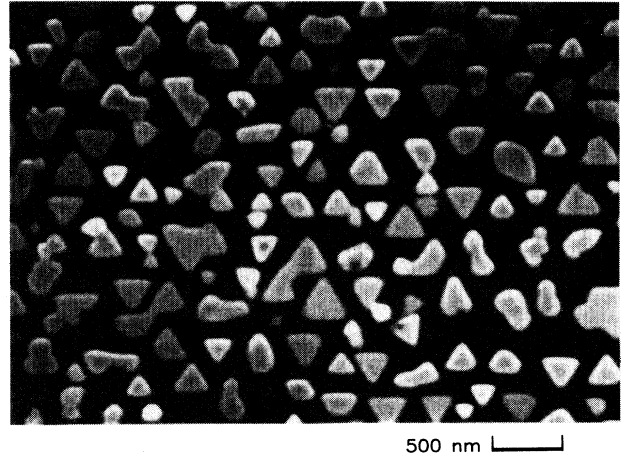


FIG. 2. Scanning electron micrograph of a heavy coverage of AgBr ( $\Theta \approx 92$ ), deposited onto Ag(111) at 125°C.

electron microscopy (SEM) in similarly prepared samples. Figure 2 is a micrograph of a high coverage of AgBr evaporated onto Ag(111) at 125°C. It is estimated that the coverage is on the order of  $\Theta \approx 92$ . The surface is found to be 38% covered with islands. This sample was shown by x-ray diffraction to have AgBr(111) ordering.

Changes in the valence-band spectra are in accordance with Stranski-Krastanov growth also. Figure 3(a) shows a series of these spectra collected at  $h\nu=55$  eV, with increasing AgBr coverage deposited at 130°C. The Ag(111)

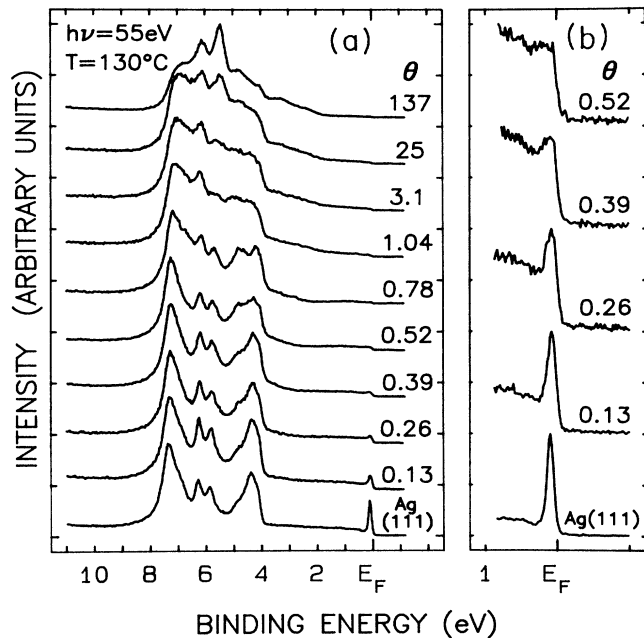


FIG. 3. (a) Valence-band and (b) surface-state normal emission ARPES spectra taken at  $h\nu=55$  eV for AgBr/Ag(111) samples prepared at 130°C. The coverages ( $\Theta$ ) are expressed as multiples of the SK break point, as indicated in Fig. 1. The experimental geometry remained as outlined in Fig. 1.

surface state is shown on an expanded scale in Fig. 3(b). The surface state is strongly attenuated by AgBr deposition and by  $\Theta=0.5$  is no longer observable. Further changes in the bulk valence band occur very slowly since a large portion of the surface remains covered only by the thin SK layer. Although the valence-band maximum,  $B^F \approx 1.8$  eV, is evident by  $\Theta=1-3$ , a Fermi edge is still observable even at  $\Theta=137$ .

LEED observations made of additional samples prepared at 130°C reveal that both the SK layer and the islands are well ordered. The  $(1 \times 1)$  Ag(111) substrate LEED spots ( $\circ$ , Fig. 4) were observed for all samples deposited at 130°C with a maximum coverage of  $\Theta=4$  being prepared in this manner. The substrate spots were also observed for the  $\Theta=10$  sample annealed to 130°C as discussed below. At  $\Theta=1.0$ , upon completion of the SK layer, a sharp  $(\sqrt{3} \times \sqrt{3})R30^\circ$  pattern (pattern A) is observed as diagrammed in Fig. 4(a). A similar LEED pattern was observed previously for light coverages of Br/Ag(111),<sup>10</sup> Cl/Ag(111),<sup>11-13</sup> and I/Ag(111).<sup>14</sup> At  $\Theta=1.5$ , an additional pattern (pattern B) coexists with the  $(\sqrt{3} \times \sqrt{3})R30^\circ$  pattern. Upon further deposition of AgBr to  $\Theta \geq 2.0$ , the  $(\sqrt{3} \times \sqrt{3})R30^\circ$  spots were no longer visible, while pattern B became stronger and sharper. In pattern B, diagrammed in Fig. 4(b), additional spots ( $\times$  and  $\blacksquare$ ) appear at  $\sim 0.3$  Ag(111) reciprocal lattice units away from the  $(1 \times 1)$  substrate spots ( $\circ$ ). Additional spots ( $\bullet$ ) are located at the vector sum of two  $0.7$  Ag(111) lattice vectors. Pattern B is not a simple  $(3 \times 3)$  pattern, but is similar to LEED patterns observed at heavier coverages of Br and Cl/Ag(111),<sup>10,11-13</sup> and seems to correspond to a superposition of oriented

Ag(111) and AgBr(111) reciprocal lattices. Note that the lattice parameters of Ag, 4.09 Å, and AgBr, 5.77 Å, have a ratio of approximately 0.7. Spots not predicted by this simple superposition ( $\times$ , Fig. 3) are best described by multiple diffraction<sup>15</sup> as proposed for Cl/Ag(111).<sup>11,12</sup> Pattern B was observed at all higher coverages prepared at 130°C and for the  $\Theta=10$  annealed sample as discussed in Sec. III C. It is interesting to note that although the photoemission surface component of the SK layer (Fig. 1) does not attenuate quickly, the  $(\sqrt{3} \times \sqrt{3})R30^\circ$  pattern is lost very rapidly. This seems to suggest the possibility that the AgBr islands are compressing the SK layer between them, thus maintaining the core level intensity but disrupting the ordering.

In summary, for AgBr depositions performed at 130°C, the photoemission results agree with the interpretation that growth is of Stranski-Krastanov type and LEED observations show both the initial SK layer and the islands to be well ordered. Due to the SK growth of AgBr deposited at 130°C, the determination of any surface reconstruction of the AgBr(111) surface has not been accomplished here. As will be discussed next, the evaporations carried out at lower temperatures and the annealing of a heavy low-temperature deposition also failed to produce a continuous film of AgBr(111). With the results presented here, however, the SK layer and AgBr(111) island components of the 130°C depositions may be separated, allowing further studies to focus on contributions originating only from the AgBr(111) islands. Additionally valuable knowledge has been gained of the temperature dependence of AgBr growth.

### B. Deposition at $-190^\circ\text{C}$

In contrast, with the substrate at  $-190^\circ\text{C}$  during the deposition, the AgBr appears to grow nearly layer-by-layer due probably to a lower AgBr surface mobility.<sup>7</sup> The Br  $3d$  core level shows only the spin-orbit-split  $3d_{5/2,3/2}$  pair. Figure 5(a) shows a series of these core levels, with increasing AgBr coverage. At low coverages,  $\Theta < 1$  the binding energies are very similar to those of the warm depositions,  $B^F = 68.05 \pm 0.05$  and  $69.06 \pm 0.05$  for the  $3d_{5/2}$  and  $3d_{3/2}$  components, respectively. However as coverage increases there is a shift of  $\sim 0.4$  eV to higher binding energy. The peak width also increases at coverages at and above  $\Theta=1.0$ , suggestive of multiple sites. (Notice the filling in of the spectral valley.) The peak width at  $\Theta < 1$  is 0.36 eV, and again is comparable to the SK component of the 130°C depositions. The width then increases to 0.51 eV for coverages at and above  $\Theta=1$ , suggestive of multiple sites. A plot of the integrated intensity of the Br  $3d$  core level peaks as a function of coverage is shown in Fig. 5(b). The Br signal increases in an exponential manner with an eventual leveling off at  $\Theta=4$ , presumably due to mean-free-path effects. In contrast to the 130°C data, no sharp break in slope is seen. This is consistent with a model of more nearly layer-by-layer growth, which is possibly due to kinetic limitations.

The LEED observations for surfaces prepared cold support this interpretation. AgBr deposition resulted

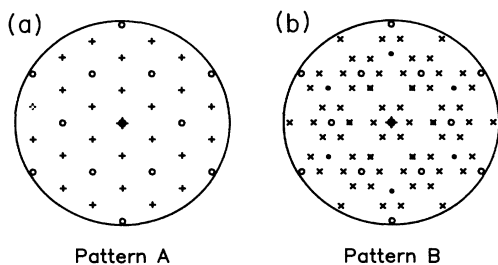


FIG. 4. Simulations of the LEED observations for the AgBr/Ag(111) samples prepared at 130°C. Beam voltage = 115 V, beam current = 1.2  $\mu\text{A}$ . (a) At the SK break point,  $\Theta=1$ , a  $(\sqrt{3} \times \sqrt{3})R30^\circ$  pattern is observed. The Ag(111)- $1 \times 1$  spots ( $\circ$ ), and  $(\sqrt{3} \times \sqrt{3})R30^\circ$  spots ( $+$ ) are shown. (b) Above the SK break point, contributions from the islands are seen. The Ag(111)- $1 \times 1$  spots ( $\circ$ ), spots consistent with single scattering from an unrotated AgBr(111)- $1 \times 1$  structure ( $\bullet$ ), and spots possibly due to multiple scattering ( $\times$ ) from both the Ag(111) and AgBr(111), are shown. Positions where AgBr(111) and multiple-scattering spots are coincident are denoted ( $\blacksquare$ ). When observing pattern B, the spots were sharp, although very weak. Often portions of the pattern were very dim and not all spots were observed. However, there was no systematic absence of spots which would be reflective of any further structural information. Also it is not unusual to observe only the first ring of multiple-scattering spots around substrate beams, as described in Ref. 13.

only in a continued blurring of the  $(1 \times 1)$  spots of the Ag substrate. No ordering of the samples deposited at  $-190^\circ\text{C}$  was observed up to  $\Theta = 10$  (the maximum coverage prepared), at which point even the substrate spots were no longer observable. The attenuation of the substrate spots at higher coverages is consistent with a reasonably homogeneous deposition, as opposed to the island growth at  $130^\circ\text{C}$ . The blurring at lower coverages and lack of any adsorbate ordering is compatible with the observation of peak broadening in the core-level photoemission, i.e., the existence of many similar, yet not identical, sites.

The valence-band photoemission observations are also in accord with the nearly layer-by-layer growth mode. Figure 6(a) contains a series of valence-band spectra, with increasing AgBr coverage, deposited at  $-190^\circ\text{C}$ . Again, the surface state, shown in Fig. 6(b), is fully attenuated by

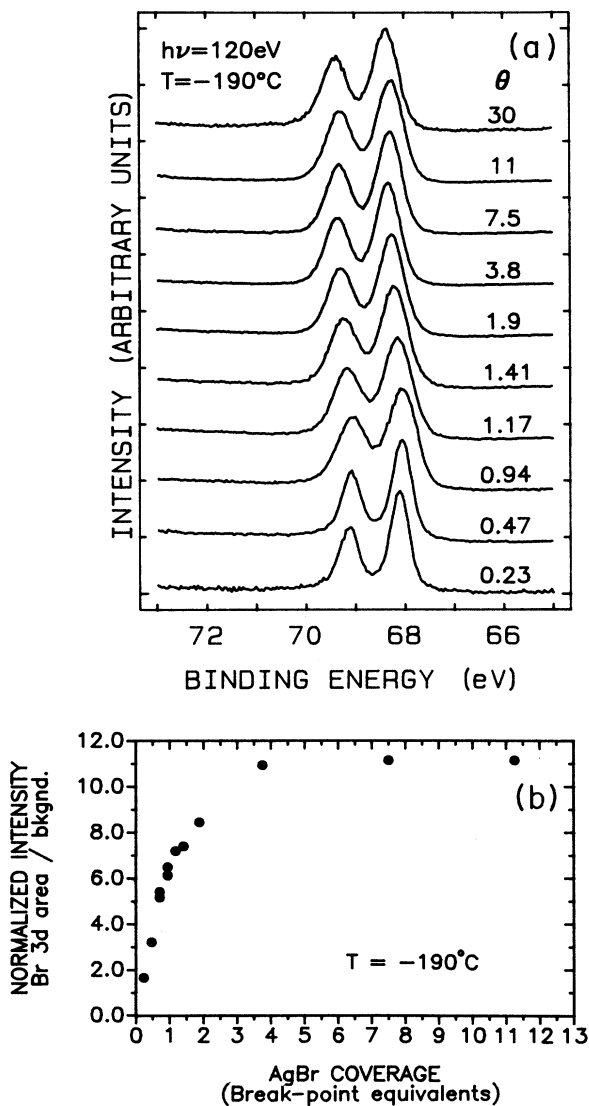


FIG. 5. Identical to Fig. 1, but for samples prepared at  $-190^\circ\text{C}$ .

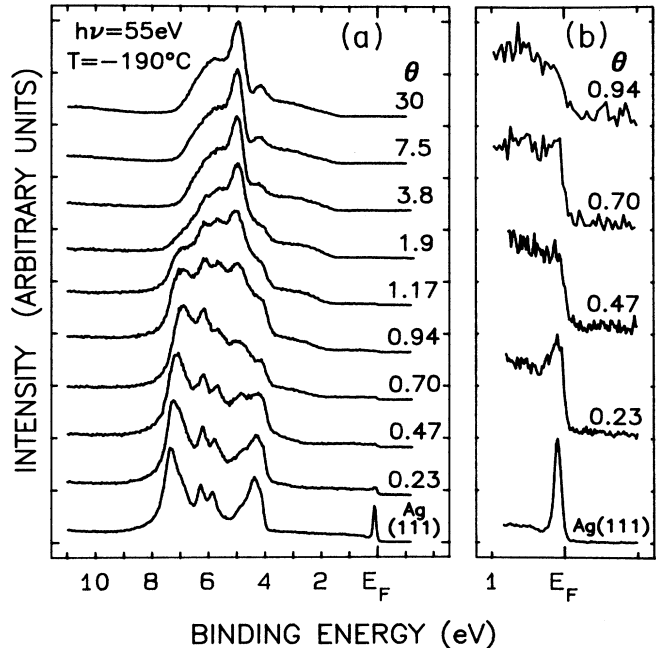


FIG. 6. Identical to Fig. 3, but for samples prepared at  $-190^\circ\text{C}$ .

$\Theta \approx 0.5$ . The valence-band spectra undergo changes with increasing coverage similar to those seen at  $130^\circ\text{C}$ , but much more rapidly. A significantly different spectrum exists at coverages as low as  $\Theta = 3$ , whereas for samples prepared at  $130^\circ\text{C}$ , coverages at least ten times greater are required to induce similar changes. The valence-band maximum again is observed at  $B^F \approx 1.8\text{ eV}$ . However, a Fermi edge cannot be observed above  $\Theta = 4$ . These results are consistent with a more uniform covering of the surface than that seen for the  $130^\circ\text{C}$  depositions.

### C. Deposition at $-190^\circ\text{C}$ with subsequent annealing

In this section it will be demonstrated that surfaces prepared cold can be converted into the  $130^\circ\text{C}$  structures, by a gentle annealing process. On two separate occasions, a cold coverage of  $\Theta = 10$  was prepared and subsequently heated in a controlled manner, once for photoemission measurements and once for LEED observations. The resulting Br  $3d$  core-level spectra are shown in Fig. 7. The bottommost spectrum is of the original cold overlayer and agrees well with those seen in Fig. 5(a). Upon warming to room temperature and being held there for 12 h, the spectrum now clearly contains four features due to two separate spin-orbit-split doublets: one at a binding energy consistent with that of the initial SK layer, and a second at a binding energy at or near that of the original cold overlayer. Upon further warming, the SK layer component remains unchanged, while the second doublet shifts to even greater binding energy, finally reaching values consistent with the ordered-AgBr(111)-island component of the  $130^\circ\text{C}$  depositions. The LEED observa-

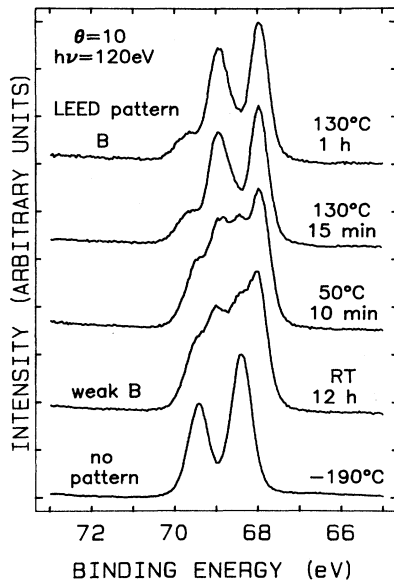


FIG. 7. Br 3d core-level, normal-emission ARPES spectra of a  $\Theta=10$  overlayer prepared at  $-190^\circ\text{C}$ , showing the evolution of components upon heating. The bottom spectrum is of the original cold overlayer. The temperature increases from bottom to top, as is indicated along with the length of time. The LEED patterns which were observed for corresponding samples are also indicated and refer to those diagrammed in Fig. 4. The experimental geometry is given in Fig. 1.

tions made on the second sample revealed that while the original cold overlayer showed no ordering, warming to room temperature produced a pattern similar to Fig. 4(b), but less well defined. Upon further heating, the pattern sharpened and the background decreased. After the final annealing to  $130^\circ\text{C}$ , a sharp pattern *B* was observed along

with extremely faint  $(\sqrt{3}\times\sqrt{3})R30^\circ$  spots within the first ring of  $\text{Ag}(111)-(1\times 1)$  spots. These  $(\sqrt{3}\times\sqrt{3})R30^\circ$  spots were not observed for the  $\Theta\geq 2$  depositions at  $130^\circ\text{C}$ . They may either have existed and not been detected due to their low intensity, or may be a result of formation of islands upon annealing which are larger but more sparsely distributed over the surface. The behavior observed in these warming experiments indicates that upon heating, the initial SK layer forms quite quickly, followed by the coalescence and ordering of the remainder of the AgBr into  $\text{AgBr}(111)$  islands.

#### IV. CONCLUSIONS

Angle-resolved-photoemission measurements and LEED observations have been used to study the growth of AgBr on  $\text{Ag}(111)$ . We have found that at  $130^\circ\text{C}$ , growth occurs in a Stranski-Krastanov manner, while at  $-190^\circ\text{C}$ , growth is more nearly layer by layer. Only the structures formed at  $130^\circ\text{C}$  show long-range order. AgBr overlayers that were prepared cold undergo a change in surface morphology upon warming, eventually reproducing spectral and diffraction features very similar to those exhibited by  $130^\circ\text{C}$  depositions.

#### ACKNOWLEDGMENTS

This work was supported by Eastman Kodak Co., Camille and Henry Dreyfus Foundation Inc., Research Corp., Rohm and Haas, Co., the donors of the Petroleum Research Foundation administered by the American Chemical Society, and the National Science Foundation (Grant Nos. DMR-8419262 and DMR-8896157). Discussions with T. Miller were enlightening and useful. The SEM micrograph of AgBr was provided by J. Timmons and D. Black of Research Laboratories, Eastman Kodak Company and was greatly appreciated.

\*Permanent address: Research Laboratories, Eastman Kodak Company, Rochester, NY 14650.

†Permanent address: Lawrence Livermore National Laboratory, Livermore, CA 94550.

<sup>1</sup>Y. Tan, F. C. Brown, C. R. A. Catlow, P. W. M. Jacobs, and L. Slifkin, *Mater. Res. Soc. Bull.* **14**, (5), 13 (1989).

<sup>2</sup>T. Tani, *Physics Today* **42**(9), 36 (1989).

<sup>3</sup>F. C. Brown, in *Treatise on Solid State Chemistry*, edited by N. B. Hannay (Plenum, New York, 1976), Vol. 4.

<sup>4</sup>G. N. Kwawer, Ph.D. thesis, University of Illinois, 1989; G. N. Kwawer, T. J. Miller, M. G. Mason, Y. Tan, F. C. Brown, and Y. Ma, *Phys. Rev. B* **39**, 1471 (1989).

<sup>5</sup>B. J. Knapp, J. C. Hansen, M. K. Wagner, W. D. Clendening, and J. G. Tobin, *Phys. Rev. B* **40**, 2818 (1989).

<sup>6</sup>Y. Tan, *Mater. Res. Soc. Bull.* **14**(5), 13 (1989).

<sup>7</sup>L. E. Brady, J. W. Castle, and J. F. Hamilton, *Appl. Phys. Lett.* **13**(2), 76 (1968); J. F. Hamilton and L. E. Brady, *Surf. Sci.* **23**, 389 (1970).

<sup>8</sup>G. E. Rhead, M. G. Barthés, and C. Argile, *Thin Solid Films* **82**, 201 (1981).

<sup>9</sup>Core-level spectra of the higher coverages taken at  $70^\circ$  off normal are also consistent with the assignment of the components to the SK layer and the islands: a decrease in intensity is observed for the layer component relative to that of the islands. This is consistent with a shadowing effect, although atomic photoelectron asymmetry and photoelectron diffraction effects must also be considered.

<sup>10</sup>P. J. Goddard, K. Schwaha, and R. M. Lambert, *Surf. Sci.* **71**, 351 (1978).

<sup>11</sup>M. Bowker and K. C. Waugh, *Surf. Sci.* **134**, 639 (1983).

<sup>12</sup>Y. Y. Tu and J. M. Blakely, *J. Vac. Sci. Technol.* **15**, 563 (1978).

<sup>13</sup>G. Rovida, F. Pratesi, M. Maglietta, and E. Ferroni, in *Proceedings of the Second International Conference on Solid Surfaces* [Jpn. J. Appl. Phys. Suppl. **2**(2), 117 (1974)].

<sup>14</sup>F. Forstmann, W. Bernt, and P. Buttner, *Phys. Rev. Lett.* **30**, 17 (1973).

<sup>15</sup>E. Bauer, *Surf. Sci.* **7**, 351 (1967); P. W. Palmberg and T. N. Rhodin, *J. Chem. Phys.* **49**, 147 (1968).

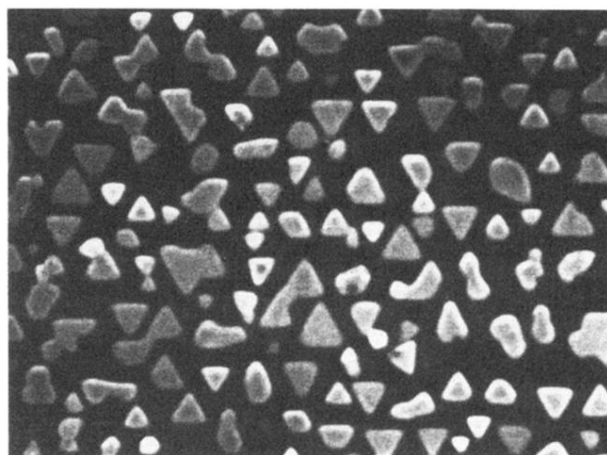


FIG. 2. Scanning electron micrograph of a heavy coverage of AgBr ( $\Theta \approx 92$ ), deposited onto Ag(111) at 125 °C.